Correlation Between Alkaline Earth Diffusion and Fragility of Silicate Glasses

ARTICLE *in* THE JOURNAL OF PHYSICAL CHEMISTRY B · AUGUST 2009

Impact Factor: 3.3 · DOI: 10.1021/jp904449t · Source: PubMed

4 AUTHORS:

Morten M Smedskjaer
Aalborg University
79 PUBLICATIONS **790** CITATIONS
SEE PROFILE

Yuanzheng Yue
Aalborg University
209 PUBLICATIONS **2,715** CITATIONS
SEE PROFILE

Joachim Deubener
Technische Universität Clausthal
109 PUBLICATIONS **1,170** CITATIONS
SEE PROFILE

Haraldur Páll Gunnlaugsson
Aarhus University
186 PUBLICATIONS **1,879** CITATIONS
SEE PROFILE

Correlation between Alkaline Earth Diffusion and Fragility of Silicate Glasses

Morten M. Smedskjaer,[†] Yuanzheng Yue,*[,†] Joachim Deubener,[‡] and Haraldur P. Gunnlaugsson[§]

Section of Chemistry, Aalborg University, DK-9000 Aalborg, Denmark, Institute of Non-Metallic Materials, Clausthal University of Technology, D-38678 Clausthal-Zellerfeld, Germany, and Department of Physics and Astronomy, University of Aarhus, DK-8000 Aarhus C, Denmark

Received: May 13, 2009; Revised Manuscript Received: June 26, 2009

We have studied the correlation between liquid fragility and the inward diffusion (from surface toward interior) of alkaline earth ions in the $SiO_2-Na_2O-Fe_2O_3-RO$ (R = Mg, Ca, Sr, Ba) glass series. The inward diffusion is caused by reduction of Fe^{3+} to Fe^{2+} under a flow of H_2/N_2 (1/99 v/v) gas at temperatures around the glass transition temperature (T_g). The consequence of such diffusion is the formation of a silica-rich nanolayer. During the reduction process, the extent of diffusion (depth) decreases in the sequence Mg^{2+}, Ca^{2+}, Sr^{2+}, and Ba^{2+}, whereas the fragility increases in the same sequence. It is found that the ratio of the activation energy of the inward diffusion E_d near T_g to the activation energy for viscous flow E_η at T_g increases with increasing fragility of the liquid. The inward cationic diffusion can be enhanced by lowering the fragility of glass systems via varying the chemical composition.

1. Introduction

Technological applications of glasses strongly depend upon the surface structure and properties. Much effort has been devoted to the development of new technologies for modifying the surface in order to enhance the physical and chemical performances of materials.[1−6] Very recently, we developed a novel method for improving surface properties of silicate glasses. This method is based on a reduction-inward diffusion route. In detail, reduction of higher valence ions to lower valence ions (e.g., Fe^{3+} to Fe^{2+}) in glasses takes places under certain types of gases at the glass transition temperature (T_g). Such reduction drives an inward diffusion (from surface toward the interior) of modifying ions, which in turn leads to the formation of a SiO_2-rich surface layer.[7] The reduction is realized via two simultaneous processes: gaseous permeation and outward flux of electron holes (see Figure 1). To maintain charge neutrality, the latter process requires an inward diffusion of mobile cations. The new surface layer considerably enhances physical and chemical performances of the glass.[7] To understand the mechanism of formation of the SiO_2-rich surface layer, it is important to study the involved cationic diffusion process.

In our previous studies, it is shown that the diffusion of alkaline earth cations from the surface to the redox front is more intense than that of alkali cations.[7,8] Here, we investigate the influence of the type of the alkaline earth ion on the inward diffusion process in the $SiO_2-Na_2O-Fe_2O_3-RO$ (R = Mg, Ca, Sr, Ba) glass series. We also attempt to find out whether and how the inward cationic diffusion is correlated with the viscous flow behavior of glasses in the glass transition range, that is, with the liquid fragility. The latter is a generally accepted concept that describes the extent of the non-Arrhenius flow.[9] The liquid fragility is related to the glass composition and structure and the glass structure strongly influences the energy barrier of the diffusion of electron holes and modifying ions. In the present work, both a kinetic fragility index m (i.e., steepness of the log viscosity vs T_g/T curve at T_g) and a thermodynamic index C_{pl}/C_{pg} (i.e., the ratio of the liquid to the glassy isobaric heat capacity at T_g) are determined as measures of liquid fragility. Finally, we also study the influence of the alkaline earth ion on the redox state of iron using Mössbauer spectroscopy because the inward cationic diffusion process is affected by the initial Fe^{3+} concentration.[7]

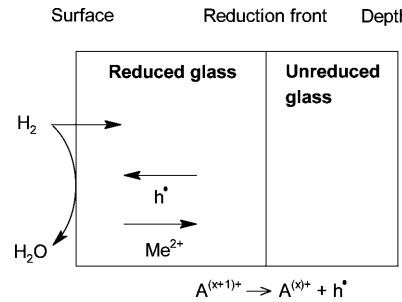

Figure 1. Schematic representation of mechanism for reduction of a polyvalent element (A). Both gaseous permeation (dissolution and diffusion) and outward (from interior toward the surface) flux of electron holes contribute to the reduction process. Me^{2+} is a network-modifying cation, $h^\bullet$ is an electron hole, and H_2 is the reducing gas molecule.

2. Experimental Section

2.1. Sample Preparation. Four iron-bearing alkali−alkaline−earth silicate glasses (see Table 1) were prepared from analytical reagent-grade SiO_2, Na_2CO_3, MgO, $CaCO_3$, $SrCO_3$, $BaCO_3$, and Fe_2O_3 powders. The mixed batch materials were melted in an electric furnace (SF6/17, Entech) at 1500 °C in a $Pt_{90}Rh_{10}$ crucible for 3 h. The melt was then cast onto a brass plate and pressed to obtain cylindrical glasses of 7−10 cm diameter and ∼5 mm height. The prepared glasses were annealed 10 K above their respective glass transition temperatures for 10 min and then cooled down to room temperature within 20 h.

* To whom correspondence should be addressed. Tel.: +45 99408522. Fax: +45 96350558. E-mail: yy@bio.aau.dk.
[†] Aalborg University.
[‡] Clausthal University of Technology.
[§] University of Aarhus.

10.1021/jp904449t CCC: $40.75
Published on Web 07/23/2009

TABLE 1: Chemical Composition, Density, Molar Volume (= Molar Mass/Density), and Iron Redox Ratio of the Prepared Glasses[a]

	chemical composition (mol %)				density	molar volume	Fe^{3+}/Fe_{tot}	r
R	SiO_2	Na_2O	Fe_2O_3[b]	RO	(g/cm^3)	(cm^3/mol)	(at%)	(Å)
Mg	69.0	7.7	1.1	21.7	2.475	20.772	74 ± 2	0.72
Ca	67.8	7.6	1.0	23.3	2.569	23.469	77 ± 2	1.00
Sr	68.6	7.7	1.0	22.4	3.022	23.498	80 ± 5	1.18
Ba	66.8	8.1	1.0	23.2	3.295	25.212	74 ± 2	1.35

[a] The radii r of the alkaline earth ions are stated for a coordination number of 6.[10] [b] All iron reported as Fe_2O_3.

2.2. Sample Characterization. The chemical compositions of the glasses were analyzed by X-ray fluorescence (S4-Pioneer, Bruker-AXS) and are listed in Table 1. The main impurity was Al_2O_3 (~0.2 mol %). Densities of the glasses were measured by He-pycnometry (Porotech) and are also given in Table 1.

Transmission ^{57}Fe Mössbauer spectroscopy on powdered samples was employed to study the effect of the alkaline earth ion on the redox state of the Fe ions. A constant acceleration spectrometer with a source of ^{57}Co in rhodium was used and calibrated with α-Fe. Measurements were made at room temperature and data were collected for one week for each sample. Isomer shifts are given relative to that of the calibration spectrum.

The glass transition temperature (T_g) was measured using a differential scanning calorimetry (DSC) instrument (STA 449C Jupiter, Netzsch). The C_p curve for each measurement was calculated relative to the C_p curve of a sapphire reference material after subtraction of a correction run with empty crucibles. Measurements were carried out in a purged Ar atmosphere. The following heating procedure was carried out to determine T_g. First, the sample was heated at 10 K/min to a temperature 1.11 times the respective T_g (in K) of each sample. Subsequently, the sample was cooled to room temperature at 10 K/min. Then, T_g was determined by a second upscan at 10 K/min according to the procedure proposed by Yue[11] in order to ensure a uniform thermal history of the four glasses. The ratio C_{pl}/C_{pg} was also determined from this scan.

To determine the kinetic fragility of the liquids, the viscosity was measured by beam-bending ($T > T_g$) and concentric cylinder ($T > T_{liquidus}$) experiments. For beam-bending experiments, bars of 45 mm length and 3 × 5 mm^2 cross-section were cut from the bulk glasses. The bars were bent in a symmetric three-point forced bending mode with 40 mm open span (VIS 401, Bähr). A 300 g weight was used to explore the viscosity range from approximately 10^{12} to 10^{10} Pa·s at a constant heating rate of 10 K/min. The viscosity was calculated according to DIN ISO 7884-4.[12] The low viscosities (<10^2 Pa·s) were measured using a concentric cylinder viscometer. The viscometer consisted of four parts: furnace, viscometer head, spindle, and sample crucible. The viscometer head (Physica Rheolab MC1, Paar Physica) was mounted on top of a high temperature furnace (HT 7, Scandiaovnen A/S). Spindle and crucible were made of $Pt_{80}Rh_{20}$. The viscometer was calibrated using the National Bureau of Standards (NBS) 710A standard glass.

2.3. Diffusion Experiments. As diffusion depths below 1 μm are expected based on our previous studies,[7,8] the sample surfaces were carefully prepared. First, the bulk glasses were cut in cylinders of 10 mm diameter and 2−3 mm height. One surface of each sample was then ground by a six-step procedure with SiC paper, followed by polishing with 3 μm diamond suspension.

To induce the inward cationic diffusion, the polished glasses were heat treated at 1 atm in an electric furnace under a flow of H_2/N_2 (1/99 v/v) gas. The presence of oxygen in the furnace is not completely avoidable. But it is possible to keep its partial pressure at a known value by using a Fe_3O_4/Fe_2O_3 redox buffer. Fe_2O_3 and Fe_3O_4 powders were mixed in the molar ratio 3:2 and placed inside the furnace together with the samples. The glass samples and redox buffer were inserted into the cold furnace and the gas-flow was turned on. The furnace was then heated at 10 K/min to the predetermined heat treatment temperature T_a and kept at this temperature for the duration t_a. The diffusion process was ended by cooling the furnace to room temperature at 10 K/min. The glasses were treated at 0.95, 1.00, 1.025, and 1.05 times their respective T_g (in K) for 2 h and at their T_g for 16 h. In addition, the Mg-containing glass was treated at its T_g for 0.5 and 8 h.

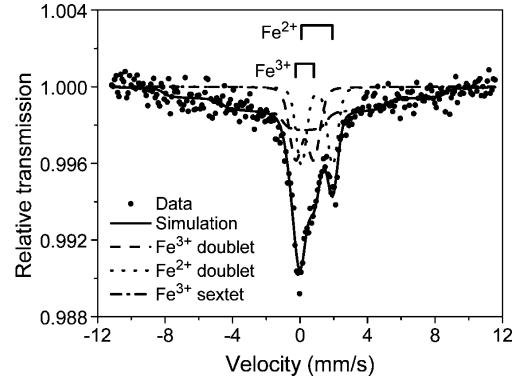

Figure 2. ^{57}Fe Mössbauer spectrum of the untreated Ca-containing glass obtained at 295 K.

The diffusion profiles were determined by electron-gas secondary neutral mass spectroscopy (SNMS). SNMS is used to determine the elemental concentrations as a function of the depth within the glass. The measurements were performed by using an INA3 (Leybold AG) instrument equipped with a Balzers QMH511 quadrupole mass spectrometer and a Photonics SEM XP1600/14 amplifier. The analyzed area had a diameter of 5 mm and was sputtered using Kr plasma with an energy of ~500 eV. The time dependence of the sputter profiles was converted into depth dependence by measuring the depth of the crater at 12 different locations on the same sample with a Tencor P1 profilometer.

3. Results

Figure 2 shows the transmission ^{57}Fe Mössbauer spectrum of the untreated Ca-containing glass at 295 K. The two doublets, seen in the spectrum, are due to paramagnetic Fe^{3+} (isomer shift of 0.28 mm/s and quadrupole splitting of 1.07 mm/s) and Fe^{2+} (isomer shift of 1.00 mm/s and quadrupole splitting of 1.86 mm/s). A sextet due to Fe^{3+} is also seen in the spectrum. It can be due to the presence of clusters that may have formed during quenching. The sextet and the two doublets appear in the Mössbauer spectra of all the four glasses; only the areas of

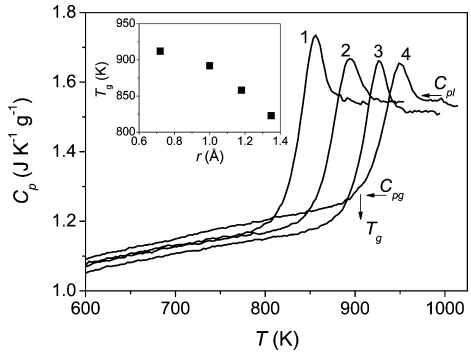

Figure 3. Glass transitions of the $SiO_2-Na_2O-Fe_2O_3-RO$ glasses with R = Mg, Ca, Sr, Ba determined by DSC at a heating rate of 10 K/min subsequent to a cooling rate of 10 K/min. Numbers correspond to R as follows: (1) Ba, (2) Ca, (3) Sr, and (4) Mg. For curve (4), the figure shows how T_g, C_{pg}, and C_{pl} are determined. Inset: The determined values of T_g as a function of the ionic radius of the alkaline earth ions (r).

TABLE 2: Characteristic Parameters of the $SiO_2-Na_2O-Fe_2O_3-RO$ Glasses with R = Mg, Ca, Sr, Ba Determined by DSC and Viscosity Measurements[a]

R	T_g(K)	C_{pl}/C_{pg}	$C_{pl}-C_{pg}$(J g^{-1} K^{-1})	F	m
Mg	912	1.22	0.28	2.68 ± 0.02	35.7 ± 0.4
Ca	892	1.27	0.32	3.00 ± 0.05	39.4 ± 0.8
Sr	858	1.29	0.35	3.30 ± 0.09	42 ± 2
Ba	823	1.30	0.36	3.55 ± 0.07	45 ± 1

[a] The errors of F and m are within the 95% confidence limits.

the peaks vary. The relative spectral areas of Fe^{3+} (doublet and sextet) and Fe^{2+} (doublet) are used to calculate the Fe^{3+}/Fe_{tot} ratio for each of the untreated glasses (Table 1).

Figure 3 shows the isobaric heat capacity (C_p) curves recorded during DSC upscans for the four glass compositions. T_g is determined at the cross point between the extrapolated straight line of the glass C_p curve before the transition zone and the tangent at the inflection point of the sharp rise curve of C_p in the transition zone. The T_g values within an accuracy of ±3 K are given in Table 2. T_g is plotted as a function of the ionic radius of the alkaline earth ion (r) in the inset of Figure 3. The radii of the alkaline earth ions are listed in Table 1 for a coordination number of 6. T_g is found to decrease with increasing r.

Figure 4 presents the viscosity data for the four compositions obtained from beam-bending and concentric cylinder viscometry. For both the low and high temperature data, a decrease in viscosity (η) with increasing r is observed.

In the literature, numerous models have been proposed to describe the temperature dependence of viscosity of glass-forming liquids.[13−18] Here, we apply the Avramov−Milchev (AM) equation[13,18−20]

$$\log \eta = A + B\left(\frac{T_g}{T}\right)^F \quad (1)$$

where A, B, F, and T_g are constants, which are obtained by fitting the viscosity data to the equation. A is $\log \eta_\infty$, where η_∞ is the viscosity at infinite temperature. F is the fragility index of the glass-forming liquid and it is a function of the chemical composition at ambient pressure.[9,18] The higher the F value is, the more fragile the liquid is. Since the viscosity for oxide glasses at T_g is equal to 10^{12} Pa·s,[11,21] eq 1 may be simplified as the following expression

$$\log \eta = \log \eta_\infty + (12 - \log \eta_\infty)\left(\frac{T_g}{T}\right)^F \quad (2)$$

In this equation, there are only three parameters. The data in Figure 4 are fitted with this modified AM equation[21] by using the Levenberg−Marquardt algorithm. It is found that eq 2 fits the data better than both the Vogel−Fulcher−Tammann (VFT) equation and the Adam−Gibbs (AG) equation.[22] The F values for the four compositions are given in Table 2. Fragility can also be described by the index m, which is defined as the slope of the log η versus T_g/T curve at T_g[23]

$$m = \left.\frac{\mathrm{d}\log\eta}{\mathrm{d}(T_g/T)}\right|_{T=T_g} \quad (3)$$

F can be converted to m through the following relation[21]

$$m = (12 - \log \eta_\infty)F \quad (4)$$

The calculated values of m are listed in Table 2 and shown in the inset of Figure 4. The studied glass melts become more fragile with increasing size of the alkaline earth ion. The fragility described here is the so-called kinetic fragility. Several attempts have been made to correlate the kinetic fragility with thermodynamic property changes at T_g.[24−27] It has been suggested to use the ratio of the heat capacity of the liquid to that of the glass at T_g (C_{pl}/C_{pg}) as a measure of thermodynamic fragility.[27] We have calculated C_{pl}/C_{pg} for the four compositions based on the DSC measurements and the values are stated in Table 2. C_{pl} is the offset value of the C_p overshoot above the glass transition range. To determine C_{pg}, a linear function is fitted to the C_p values at temperatures below T_g. The value of this function at T_g is reported as C_{pg}. The results in Table 2 show that C_{pl}/C_{pg} increases with increasing r. For comparison, the step change in the heat capacity ($C_{pl}-C_{pg}$) at the glass transition is also calculated and listed in Table 2. Similar tendencies for C_{pl}/C_{pg} and $C_{pl} - C_{pg}$ are observed.

Figure 5a−d illustrates the diffusion profiles in the four glasses heat treated under H_2/N_2 (1/99) at their respective T_g for 16 h. All glasses display a depletion of sodium, iron, and

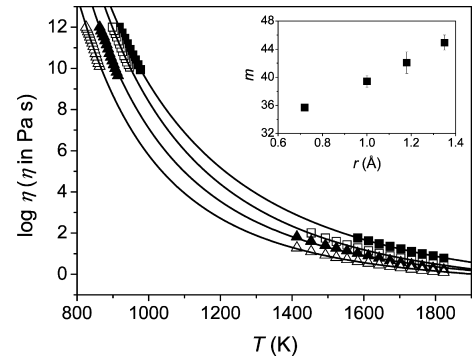

Figure 4. Dependence of viscosity on temperature of the $SiO_2-Na_2O-Fe_2O_3-RO$ glasses with R = Mg, Ca, Sr, Ba. Closed squares, R = Mg; open squares, R = Ca; closed triangles, R = Sr; open triangles, R = Ba. The data are fitted with eq 2 and the values of the fitting parameter F are listed in Table 2. The low- and high-temperature viscosity data have been measured by beam-bending and concentric cylinder viscometry, respectively. Inset: The fragility index m determined by eq 4 as a function of the ionic radius of the alkaline earth ions (r).

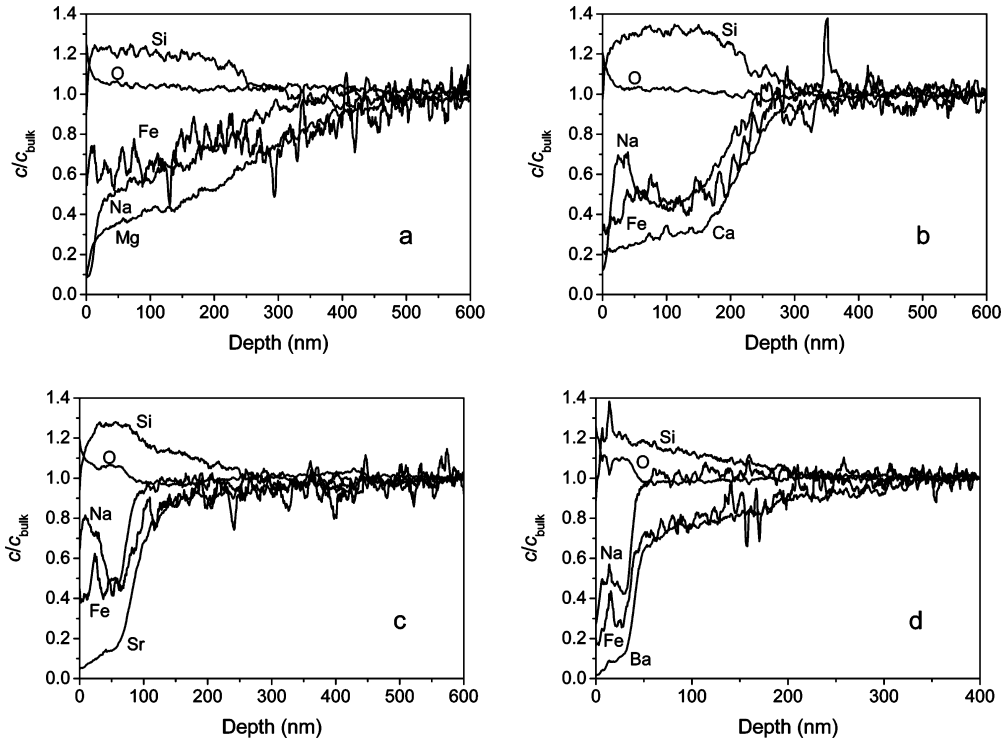

Figure 5. SNMS depth profiles of the $SiO_2-Na_2O-Fe_2O_3-RO$ glasses with R = Mg, Ca, Sr, Ba heat treated at their respective T_g for 16 h in H_2/N_2 (1/99). The letters on the figure correspond to R as follows: (a) Mg, (b) Ca, (c) Sr, and (d) Ba. The curves are plotted as concentration of the element at a given depth divided by the concentration of the same element in the bulk of the glass (c/c_{bulk}).

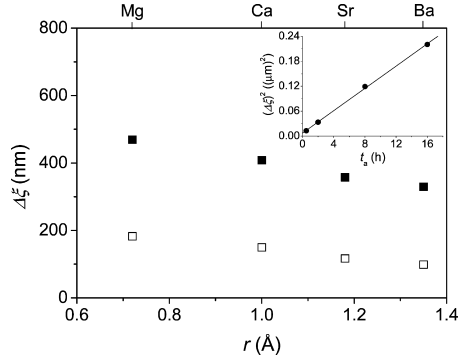

Figure 6. Diffusion depths ($\Delta\xi$) of the alkaline earth ions as a function of the ionic radius r. The glasses have been heat treated in H_2/N_2 (1/99) at their respective T_g for different durations (t_a). Closed squares, t_a = 16 h; open squares, t_a = 2 h. Inset: Plot of $(\Delta\xi)^2$ against t_a (0.5, 2, 8, and 16 h) at $T_a = T_g$ for the Mg-containing glass.

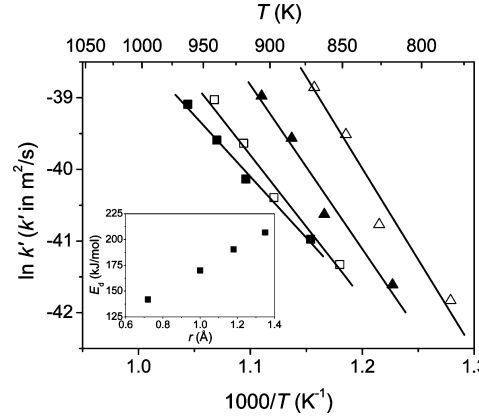

Figure 7. Arrhenius plot of ln k' as a function of the reciprocal absolute temperature of the $SiO_2-Na_2O-Fe_2O_3-RO$ glasses with R = Mg, Ca, Sr, Ba heat treated in H_2/N_2 (1/99) at different conditions. Closed squares, R = Mg; open squares, R = Ca; closed triangles, R = Sr; open triangles, R = Ba. Inset: The corresponding activation energies of diffusion (E_d) as a function of the ionic radii of the alkaline earth ions (r).

the respective alkaline earth ion near the surface. This inward diffusion causes the high surface concentration of silica. It should be noted that the untreated glasses show no changes in composition as a function of depth.

To quantitatively analyze the data, the diffusion depths ($\Delta\xi$) of the alkaline earth ions are determined for $T_a = T_g$ (Figure 6). $\Delta\xi$ is calculated as the first depth at which $c/c_{bulk} \geq 1$ for three measurements in succession. Figure 6 shows that the order of the alkaline earth ion mobility at isokom temperatures is $Mg^{2+} > Ca^{2+} > Sr^{2+} > Ba^{2+}$.

For the reduction mechanism presented in Figure 1 to be valid, chemical diffusion of the alkaline earth ions must occur, that is, the diffusion must be parabolic with time. Parabolic kinetics can be expressed in its integrated form as[28]

$$(\Delta\xi)^2 = k't \qquad (5)$$

where t is time and k' is a constant. k' is proportional to the product of the diffusion coefficient of the rate-limiting species and the normalized (to RT) thermodynamic driving force. A kinetic analysis is performed by plotting $(\Delta\xi)^2$ against the duration of the heat treatment (0.5, 2, 8, and 16 h) at $T_a = T_g$ for the Mg-containing glass. A linear relationship is found with a coefficient of determination (R^2) of 0.999 (see inset of Figure 6). This proves that the kinetic signature is indeed parabolic.

To study the temperature dependence of the alkaline earth diffusion, we calculate the temperature sensitivity of k' from the change of $\Delta\xi$ with temperature at a constant diffusion time. Figure 7 presents the resulting Arrhenius plots. The diffusion data for each glass reveal an Arrhenius dependence on temperature (see solid lines in Figure 7). From the slope of each line,

an activation energy of diffusion around T_g (E_d) is calculated and shown as a function of r in the inset of Figure 7. E_d increases with increasing r, and hence, with decreasing field strength of the alkaline earth ions.

4. Discussion

Since only the nature of the alkaline earth ion has been changed and not its concentration, the number of non-bridging oxygens (NBOs) is the same in all glasses when neglecting the small variations in the compositions of the glasses (Table 1). As it is known, variation of the fragility of silicate melts may result from small changes of hydroxyl content.[29] However, differences in hydroxyl content are predominantly due to variations of the melting conditions, which are not modified for the silicate glasses of this study. Thus, we assume only marginal changes in hydroxyl concentration of the untreated glasses. In addition, the iron redox ratio does not differ between the samples when considering the error range of the data (see Table 1), which is in agreement with the findings in a previous study.[30] Hence, the observed changes in T_g, fragility, and diffusion cannot be explained by the concentration of NBOs or Fe^{3+}. The changes must be due to the difference in size of the alkaline earth ions (and hence, in their field strength), in ionic packing density, and bond angle distributions.

The increase in T_g with decreasing r of alkaline earth ions (R^{2+}) is attributed to the strengthening of the overall network since a decrease of r also leads to an increase in their field strength, and hence, to an enhanced attraction of R^{2+} ions to their surrounding structural groups of [SiO_4] tetrahedra. The Mg^{2+} ions most strongly attract the nearby [SiO_4] tetrahedra, and hence, a higher potential energy barrier needs to be overcome to initiate glass transition. This finding is in agreement with that of Natrup and Bracht.[31] Similarly, the viscosity decreases at both high and low temperatures with increasing r.[32] In accordance with the alkaline earth field strength also the molar volume of the glasses decreases in the sequence Ba > Sr > Ca > Mg, indicating a less open structure for high field strength cations (Table 1).

The kinetic fragility (quantified by F or m) shows a positive correlation with the thermodynamic fragility (quantified by C_{pl}/C_{pg} or $C_{pl}-C_{pg}$). This agrees with the observations by other authors.[33,34] However, it has been shown that this correlation is not generally true for small organic and polymeric liquids, whereas the correlation exists for inorganic glass-forming liquids.[27] The fragility is found to increase with increasing r of the alkaline earth ions in the glass series studied in this work (see Figure 4). This may be explained as follows. For a more fragile liquid, there is a larger change in the structure of the liquid with temperature than for a less fragile liquid. The high field strength of Mg^{2+} causes a high degree of short-range order, which prevents the structure from a rapid breakdown with increasing temperature.

Our diffusion experiments have shown that the Mg^{2+} ions are the fastest at isokom temperatures and have the lowest E_d. It has previously been reported that alkaline earth ions are most mobile in alkali alkaline earth silicate glasses when the radii of the alkali and alkaline earth ions are similar.[35−37] The jump of an alkaline earth ion from one octahedral site to another leaves behind a high negative charge density that induces an electric dipole moment. This moment might cause a backward jump of the alkaline earth ion. However, when the alkali and alkaline earth ions have similar radii, the highly mobile alkali ions can easily enter the alkaline earth ion sites and hereby reduce the probability of the backward jump. In our sodium alkaline earth silicate glasses, the Ca^{2+} ions should then be the fastest and have the lowest E_d as the radius of Na^+ (1.02 Å) is very similar to that of Ca^{2+} (1.00 Å). The glasses studied by Natrup and co-workers[36,37] contain the same atomic concentration of alkali and alkaline earth ions, whereas our glasses contain ~45% more alkaline earth than alkali ions. In addition, the iron reduction causes the alkali ions to diffuse (role of Na^+ in diffusion process is discussed later). These factors limit the ability of Na^+ to jump into the empty alkaline earth ion sites, which might explain why Ca^{2+} is not found to be the fastest ion in our glasses.

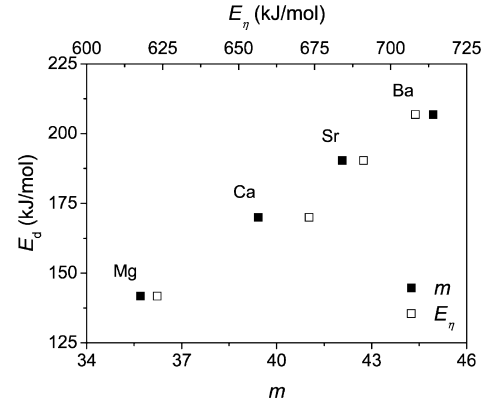

Figure 8. Activation energy of diffusion around T_g (E_d) versus the fragility index m determined by eq 4 and the activation energy of viscous flow at T_g (E_η) determined by eq 6.

To account for our experimental observations, we instead consider the modified random network (MRN) model for glasses proposed by Greaves.[38] According to the MRN model, the network modifying oxides form interconnected channels (i.e., a percolative network) at sufficiently high concentration. The threshold for percolation occurs at 16 vol % of modifying oxides,[39] which is exceeded by the glass compositions studied in this work. The alkaline earth ions should diffuse fastest through the channels when their size is smallest, which explains our diffusion results at isokom temperatures. The activation energy of diffusion is the sum of an electrostatic term due to the Coulomb interaction between the cation and the NBO plus an elastic part to open up doorways into neighboring sites.[40] In our glasses, the latter term governs the activation energy as the smallest alkaline earth ion has the lowest E_d since it most easily moves through the channels. The channels are constituted by [SiO_4] tetrahedra, that is, the required displacement of oxygen is relatively small for a small alkaline earth ion.

To study the link between ionic diffusion and fragility, E_d is plotted against m in Figure 8. m is found to be proportional to E_d, implying that the diffusion of alkaline earth ions in glasses is related to the liquid fragility. This could be explained as follows. Strong glass systems have a smaller configurational entropy (S_c) than fragile glass systems. S_c is the part of the entropy of a pure liquid that is determined by the abundance of possible packing states obtainable at the temperature T.[24] Therefore, fragility depends on the multiplicity of states (local potential energy minima),[41,42] that is, strong systems will have a structure with fewer accessible states than fragile systems.[41] Alkali and alkaline earth ions should therefore diffuse faster in strong systems than in fragile systems due to the simple diffusion paths in the former ones.

To study if the diffusion of alkaline earth ions in glasses is linked to the viscous flow of the network, the following relation is considered[21]

$$E_\eta = mT_gR \ln 10 = (12 - \log \eta_\infty)FT_gR \ln 10 \quad (6)$$

where E_η is the activation energy of viscous flow at T_g and R is the gas constant. E_d is plotted against E_η in Figure 8 and a clear linear correlation is observed, but the E_d/E_η ratio is smaller than 1. According to the Stoke−Einstein equation, the activation energy of diffusion increases with increasing viscosity. However, the equation cannot be used to predict ion mobilities, because the ions use the transportation route with the lowest activation energy, that is, they flow faster than the cooperative rearrangements of the structural units. In other words, the diffusion of alkali and alkaline earth ions is decoupled from the network change.

The decoupling ratio E_d/E_η at T_g is calculated for each of the four glasses and is listed in Table 3. It seems that with increasing fragility the degree of decoupling decreases, that is, the ratio increases. Previously, the network relaxation (α-relaxation) and the fast β- and γ-relaxations have been explored for sodium trisilicate (NS3) glasses[43] and photo-thermorefractive (PTR) glass.[44] The origin of γ-relaxation is believed to be the single ion diffusion of network modifying cations.[45,46] In mixed alkali alkaline earth silicate glasses, Roling[47] has suggested that besides water (as OH) interaction, interdiffusion of alkali and alkaline earth ions is the cause of the β-relaxation. The decoupling ratios E_β/E_α and E_γ/E_α at T_g for the NS3 and PTR glasses are stated in Table 3. Comparison of these ratios with the E_d/E_η ratios determined in this work indicates that an interdiffusion mechanism of alkaline earth ions with sodium ions occurs in the studied glasses.

The role of Na^+ in the diffusion processes appears to be complex. Even though alkali ions are normally considered to be the fastest ions in glasses,[48,49] the diffusion depth of Na^+ is generally smaller than that of the alkaline earth ions, which is in agreement with our previous studies.[7,8] In addition, an enrichment peak of Na^+ (compared to the surrounding Na^+ concentration) is found near the surface of the heat treated samples for R = Ca, Sr, and Ba, but not for R = Mg (Figure 5). The height and width of this peak decrease with decreasing T_a and t_a. These results imply that Na^+ diffuses back to the surface after its initial inward diffusion. This agrees with the existence of an interdiffusion mechanism of alkaline earth ions and sodium ions as suggested by the values of the decoupling ratios. These issues will be addressed in more detail in a future study by investigating the reduction induced diffusion in $68SiO_2-23CaO-8R_2O$ (R = Na, K, Rb, Cs)$-1\ Fe_2O_3$ glasses.

Other features of the inward cationic diffusion process are discussed in the following. The diffusion profiles presented in Figure 5 indicate that the diffusion of Ca^{2+}, Sr^{2+}, and Ba^{2+} occurs in different step, whereas this is not the case for Mg^{2+}. For the Mg-containing glass, the change in concentration with depth is approximately linear. The inward diffusion of Ca^{2+}, Sr^{2+}, and Ba^{2+} might be slowed down at larger depths due to the accumulation of these relatively large ions. This would explain why the depth, at which the slope of the concentration versus depth curve suddenly changes, seems to decrease with increasing r (see Figure 5).

The inward diffusion process is driven by reduction of Fe^{3+} to Fe^{2+}, but Fe^{2+} is capable of diffusing itself. The ionic radius of Fe^{2+} in 6-fold coordination is 0.78 Å for the high spin state.[10] The diffusion data of iron reveal two general features. First, the diffusion depth of Fe^{2+} decreases with increasing r. Second, the ratio between the diffusion depth of Fe^{2+} and that of the alkaline earth ion ($\Delta\xi_{Fe}/\Delta\xi_R$) decreases with increasing r (on average, 0.9 for R = Mg and 0.4 for R = Ba). These observations are explained by the steric hindrance induced by the larger alkaline earth ions on the diffusion of Fe^{2+}.

TABLE 3: Fragility m and Decoupling Ratio E_d/E_η at T_g of the $SiO_2-Na_2O-Fe_2O_3-RO$ Glasses with R = Mg, Ca, Sr, Ba[a]

glass	m	E_d/E_η	E_β/E_α	E_γ/E_α	reference
R = Mg	35.7	0.227			this work
R = Ca	39.4	0.253			this work
R = Sr	42	0.276			this work
R = Ba	45	0.292			this work
PTR	32.6		0.253	0.155	Deubener et al.[44]
NS3	42.9		0.302	0.132	Deubener et al.[43]

[a] m and the decoupling ratios E_β/E_α and E_γ/E_α at T_g of a photo thermorefractive (PTR) and a sodium trisilicate (NS3) glass are also stated for comparison. The PTR glass is a sodium zinc aluminosilicate glass doped with fluorine, bromine, cerium, silver, antimony, and tin.

5. Conclusions

By means of an inward diffusion process driven by reduction of iron, we have studied the diffusion of alkaline earth ions in the glass transition range in silicate glasses and the link to the liquid fragility. The fragility is found to increase with increasing ionic radius of the alkaline earth ion. The diffusion is studied by heat treating the glasses at temperatures around T_g as this causes an inward diffusion of mobile cations due to reduction of Fe^{3+} to Fe^{2+}. The determined activation energies of diffusion (E_d) reveal that the small alkaline earth ions are the most mobile and that E_d increases with increasing fragility. We have explained our results based on the modified random network model, which predicts the formation of percolation channels in the studied glasses. The small ions most easily move through these channels that are constituted by [SiO_4] tetrahedra. The results imply that the inward cationic diffusion can be enhanced by lowering the fragility of glass systems. In accordance with the diffusion mechanism, it is found that $E_d < E_\eta$ as the alkaline earth ions bypass the slow cooperative rearrangements of the glass network by using the transportation path with the lowest activation energy. The decoupling ratio E_d/E_η at the glass transition is found to increase with increasing fragility. The inward cationic diffusion process can be used to create a silica-rich nanolayer on glass surfaces, and the results obtained in this study show that Mg^{2+} ions most effectively creates this layer at isokom temperatures.

Acknowledgment. We thank T. Peter and M. Zellmann (Clausthal University of Technology) for experimental assistance. We also thank R. Keding, M. Moesgaard, and M. Jensen (Aalborg University) for valuable discussions. This work was supported by the International Doctoral School of Technology and Science at Aalborg University under Ph.D. stipend No. 562/06-FS-28045.

References and Notes

(1) Dunken, H. *J. Non-Cryst. Solids* **1991**, *129*, 64.
(2) Saggioro, B. Z.; Ziemath, E. C. *J. Non-Cryst. Solids* **2006**, *352*, 2783.
(3) Chen, F.; Wang, X. L.; Wang, K. M. *Opt. Mater.* **2007**, *29*, 1523.
(4) Akiba, S.; Hara, W.; Watanabe, T.; Matsuda, A.; Kasahara, M.; Yoshimoto, M. *Appl. Surf. Sci.* **2007**, *253*, 4512.
(5) Varshneya, A. K. *Fundamentals of Inorganic Glasses*; Society of Glass Technology: Sheffield, England, 2006.
(6) Shelby, J. E. *Introduction to Glass Science and Technology*; The Royal Society of Chemistry: Cambridge, England, 2005.

(7) Smedskjaer, M. M.; Yue, Y. Z. *J. Non-Cryst. Solids* **2009**, *355*, 908.
(8) Smedskjaer, M. M.; Deubener, J.; Yue, Y. Z. *Chem. Mater.* **2009**, *21*, 1242.
(9) Angell, C. A. *Science* **1995**, *267*, 1924.
(10) Shannon, R. D. *Acta Crystallogr.* **1976**, *A32*, 751.
(11) Yue, Y. Z. *J. Non-Cryst. Solids* **2008**, *354*, 1112.
(12) DIN ISO 7884−4, *Viskosität und viskosimetrische Festpunkte. Teil 4: Bestimmung der Viskosität durch Balkenbiegen*, 1987.
(13) Avramov, I. *J. Non-Cryst. Solids* **1998**, *238*, 6.
(14) Vogel, H. *Z. Phys.* **1921**, *22*, 645.
(15) Fulcher, G. S. *J. Am. Ceram. Soc.* **1925**, *8*, 339.
(16) Tammann, G.; Hesse, W. *Z. Anorg. Allg. Chem.* **1926**, *156*, 245.
(17) Adam, G.; Gibbs, J. H. *J. Chem. Phys.* **1965**, *43*, 139.
(18) Avramov, I. *J. Non-Cryst. Solids* **2005**, *351*, 3163.
(19) Milchev, A.; Avramov, I. *Phys. Status Solidi B* **1983**, *120*, 123.
(20) Avramov, I. *J. Mater. Sci. Lett.* **1994**, *13*, 1367.
(21) Yue, Y. Z. *J. Non-Cryst. Solids* **2009**, *355*, 737.
(22) Solvang, M.; Yue, Y. Z.; Jensen, S. L.; Dingwell, D. B. *J. Non-Cryst. Solids* **2004**, *336*, 179.
(23) Angell, C. A. *J. Non-Cryst. Solids* **1991**, *131−133*, 13.
(24) Martinez, L.-M.; Angell, C. A. *Nature* **2001**, *410*, 663.
(25) Wang, L. M.; Angell, C. A.; Richert, R. *J. Chem. Phys.* **2006**, *125*, 074505.
(26) Roland, C. M.; Santangelo, P. G.; Robertson, C. G.; Ngai, K. L. *J. Chem. Phys.* **2003**, *118*, 10351.
(27) Huang, D. H.; McKenna, G. B. *J. Chem. Phys.* **2001**, *114*, 5621.
(28) Schmalzried, H. *Solid State Reactions*; Verlag Chemie: Weinheim, Germany, 1984.
(29) Deubener, J.; Behrens, H.; Müller, R.; Zietka, S.; Reinsch, S. *J. Non-Cryst. Solids* **2008**, *354*, 4713.
(30) Bingham, P. A.; Parker, J. M.; Searle, T.; Williams, J. M.; Smith, I. *C. R. Chimie* **2002**, *5*, 787.
(31) Natrup, F. V.; Bracht, H. *Phys. Chem. Glasses* **2005**, *46*, 95.
(32) Hess, K.-U.; Dingwell, D. B.; Webb, S. L. *Eur. J. Mineral.* **1996**, *8*, 371.
(33) Angell, C. A. In *Relaxation in Complex Systems*; Ngai, K. L., Wright, G. B., Eds.; USGPO: WA, 1985; pp. 3−41.
(34) Hornbøll, L.; Yue, Y. Z. *J. Non-Cryst. Solids* **2008**, *354*, 1862.
(35) Roling, B.; Ingram, M. D. *Solid State Ionics* **1998**, *105*, 47.
(36) Natrup, F.; Bracht, H.; Martiny, C.; Murugavel, S.; Roling, B. *Phys. Chem. Chem. Phys.* **2002**, *4*, 3225.
(37) Martiny, C.; Murugavel, S.; Roling, B.; Natrup, F.; Bracht, H.; Ingram, M. D. *Glass. Technol.* **2002**, *43C*, 309.
(38) Greaves, G. N. *J. Non-Cryst. Solids* **1985**, *71*, 203.
(39) Zallen, R. *The Physics of Amorphous Solids*; Wiley: New York, 1983.
(40) Anderson, O. L.; Stuart, D. A. *J. Am. Ceram. Soc.* **1954**, *37*, 573.
(41) Sastry, S. *Nature* **2001**, *409*, 164.
(42) Speedy, R. J. *J. Phys. Chem. B* **1999**, *103*, 4060.
(43) Deubener, J.; Yue, Y. Z.; Bornhöft, H.; Ya, M. *Chem. Geol.* **2008**, *256*, 298.
(44) Deubener, J.; Bornhöft, H.; Reinsch, S.; Müller, R.; Lumeau, J.; Glebova, L. N.; Glebov, L. B. *J. Non-Cryst. Solids* **2009**, *355*, 126.
(45) George, A. M.; Stebbins, J. F. *Am. Mineral.* **1998**, *83*, 1022.
(46) Gruener, G.; Odier, P.; De Sousa Meneses, D.; Florian, P.; Richet, P. *Phys. Rev. B* **2001**, *64*, 024206.
(47) Roling, B. *Curr. Opin. Solid State Mater. Sci.* **2001**, (5), 203.
(48) Natrup, F.; Bracht, H.; Murugavel, S.; Roling, B. *Phys. Chem. Chem. Phys.* **2005**, *7*, 2279.
(49) Nijokep, E. M. T.; Mehrer, H. *Solid State Ionics* **2006**, *177*, 2839.

JP904449T